Systems and Computers in Japan, Vol. 35, No. 6, 2004
Translated from Denshi Joho Tsushin Gakkai Ronbunshi, Vol. J85-D-II, No. 3, March 2002, pp. 483 –492

Transformation from Population Codes to Firing Rate Codes by Learning: Neural Representation of Smooth Pursuit Eye Movements

Shinya Taguchi,[1,2] Hiromitsu Tabata,[1,3] Tomohiro Shibata,[4] and Mitsuo Kawato[1,2]

[1]Nara Institute of Science and Technology, Ikoma, 630-0101 Japan

[2]Department 3, Human Information Science Laboratories, ATR, Kyoto, 619-0288 Japan

[3]National Institute of Advanced Industrial Science and Technology, Tsukuba, 305-8568 Japan

[4]Creating the Brain, CREST, Japan Science and Technology Corporation, Kyoto, 619-0288 Japan

SUMMARY

It has been reported that not only the information related to retinal slip but also the non-visual information were population-coded in the middle temporal (MT) area and the medial superior temporal (MST) area during smooth pursuit eye movements. On the other hand, it has been also reported that the information related to motor signals to generate eye movements were firing rate-coded in the Purkinje cells in the cerebellum. Here, we propose a computational model of smooth pursuit that includes various temporal patterns of neural firing in the MT/MST areas and synaptic plasticity in the cerebellar cortex. We show that the signals to generate smooth pursuit eye movements could be extracted from the signals population-coded in the cerebral cortex by means of the synaptic plasticity in the cerebellar cortex. Our results indicate that the transformation from population codes to firing rate-codes occurs in the cerebellum during smooth pursuit eye movements © 2004 Wiley Periodicals, Inc. Syst Comp Jpn, 35(6): 79–88, 2004; Published online in Wiley InterScience (www.interscience.wiley.com). DOI 10.1002/scj.10322

Key words: smooth pursuit eye movements; population codes; firing rate codes; feedback error learning.

1. Introduction

First, we define population coding and firing rate coding (scalar coding) in terms of terminology.

[Population coding]

When cells have a preferred stimulus, the firing rate of the cells decreases monotonously as the input is away from the preferred stimulus. We define population coded information as the information represented in cell groups having various preferred stimuli.

[Firing rate coding] (scalar coding)

We define firing rate coded information as the information that is in a monotonously increasing or decreasing relationship to the firing rate of cells varying temporally.

In the study of population coding, there are problems regarding transformation of an external stimulus into the activity distribution of a cell group, transformation from the

activity distribution of a cell group to recognition and motor information, and how these transformations are optimal. There are many theoretical, physiological, behavioral, and psychological studies related to population coding, i.e., theoretical analyses [l], firing dynamics of neurons in MT area [2], adaptation to visual stimuli given in a multiple number of directions in MT and MST area [3], winner-take-all methods [4], vector averaging methods in Ml [5], and classifications of these methods by their application according to circumstances [6]. To understand how the brain processes population coded information, it is inevitable to construct a computational model that can reproduce these physiological, behavioral, and psychological data in detail. However, so far, most of the theoretical studies were top-down and were not able to reproduce the experimental data in detail. The bottom-up approaches that narrow down computational theory or population coding algorithms by modeling study connecting to the physiological, behavioral, and psychological experiments are necessary.

It appears that smooth pursuit eye movements are appropriate for population code studies for the following advantages: (1) The relationship between inputs and outputs is clear and it can be treated as a system of one degree of freedom. (2) The signal processing pathway related to the smooth pursuit is clarified by previous physiological experiments. (3) A computational theory that adaptation of the eye movements can be explained by the plasticity in the cerebellar cortex has been proposed, and the theory has been supported by physiological experiments [8]. Therefore, we model the transformation from visual information to motor information on the basis of this theory. Here, we investigate how the motor information is extracted from population coded visual information from a viewpoint of smooth pursuit eye movements.

We outline previous studies on the computational theory and physiological experiments of the eye movements in Section 2. We propose a simple model and a more physiologically plausible model in Section 3. We show simulation results in Section 4. We examine the reasonableness and the problems of the models in Section 5.

2. Previous Studies on Computational Theory and Physiological Experiments on Eye Movement System

The neural circuits related to OFR (ocular following responses) [9] and smooth pursuit eye movements [7, 9] have been physiologically studied. There are neurons having various speed and direction selectivities in the MT and MST areas, and the information related to visual motion is population-coded [2, 10, 11]. During smooth pursuit, the cells in the MTf area (the foveal region of the MT area) and a part of the MSTI area (a lateral-anterior region of the MST area) have signals related to visual inputs (retinal error) and the cells in the MST area also have signals related to signals independent of visual inputs (extraretinal signals).

Lisberger and Movshon [2] have shown that the velocity and the acceleration of a visual stimulus are population-coded in the MT area by their recording study in anesthetized monkeys. They found that a temporal waveform approximately proportional to the target velocity or acceleration was calculated by a linear sum of the temporal waveform of the firing rate in each cell.

On the other hand, a simple spike of Purkinje cells in the cerebellum has a simple proportional ratio with the linear sum of the acceleration, velocity, and position of the eye movement, and has two-directional selectivity, i.e., downward and ipsilateral. In other words, the information to generate the eye movement is possibly firing rate-coded in the Purkinje cells [13, 14]. It has been suggested that visual information population-coded in the MT and the MST areas is transformed into the motor information firing rate-coded in the Purkinje cells [15].

Yamamoto et al. [16] proposed computational model of the OFR based on the framework of the feedback error learning theory [22]. In their model, transformation from sensory information into motor information is obtained by the synaptic plasticity between Purkinje cells and parallel fibers. This result indicates that the cerebellum obtains an inverse dynamics model to control eye movement. This model has been supported by physiological experiments [13, 14, 17].

However, the model proposed by Yamamoto et al. includes only three kinds of temporal waveforms of the firing rate in the MST area. Accordingly, their model is insufficient to describe physiological properties in the MST area. In addition, in their simulation, the firing rate pattern of the Purkinje cells is obtained only by simple ensemble of the firing rate waveforms in the MST area. Therefore, it is still obscure how the signals to generate eye movements are extracted from visual related information population-coded in the MST area. Furthermore, they assumed a linear filter as the neural circuit from the cerebellum to the eye (referred to as a plant below). It is necessary to test other kind of plants in order to address the question how the information appropriate to each plant extracts from the visual related information population-coded in the MST area through learning in the cerebellum.

In Lisberger and Movshon [2], the eye movements of the monkeys were not induced due to anesthesia. The temporal waveforms of the firing rate of the MT area should vary in many ways if the eye movements occur, and how the activity distribution of a cell group changes or how a human or a monkey learns weighting has not been addressed.

In the next section, we designed the model of smoother pursuit eye movement based on the computational theory and physiological experiments described above. We assume that the neurons in the MT and the MST areas included various temporal patterns of firing rate under the condition that eye movements could be induced. Then, we conduct the computer simulation to investigate whether the appropriate signals to generate eye movements could be extracted from the cell population in the MT and the MST areas.

3. Models

3.1. Nomenclature

The following symbols are used.

t: time (ms)

N: total number of the cells in MT and MST, respectively

i: index of MT, MST area cells ($1 < i < N$)

$S(t)$: simple spike of Purkinje cells

$E(t)$: eye speed or velocity (deg/s)

$T(t)$: visual target velocity (deg/s)

$x_i(t)$: firing rate of i-th MT, MST area cell

w_i: synapse weight between parallel fiber and Purkinje cell having $x_i(t)$ as input

$\mathbf{w}$: weight vector having w_i as components

$y(t)$: climbing fiber input

ε: learning coefficient in feedback error learning

Δ_1: delay time of the cells in the MT, MST area before firing (ms)

Δ_2: delay time from the firing of a simple spike until the start of eye movement (ms)

δ_1: delay in time when the parallel fiber input and the climbing fiber input are multiplied in learning (ms)

δ_2: latent time of climbing fiber input (ms)

$\mathcal{L}$: Laplace transform operand

K: $= (as + 1)/((bs + 1)(cs + 1))$, where $a = 83$ ms, $b = 16$ ms, $c = 179$ ms [18]

M: number of kinds of sample target velocities when an optimal weight is computed

m: index of sample target velocity when an optimal weight is computed ($1 < m < M$)

p, q: kind of plant; $p, q \in \{1, 1/s, K\}$

P: linear filter showing a plant

$\mathbf{b}_p$: ideal motor command when plant is p

J: evaluation function determining $\mathbf{w}$ for outputting an ideal motor command

I: unit square matrix

k: coefficient of normalization term of J

$\tilde{w}_i^p$: weight of i-th synapse that minimizes J when plant is p

$\tilde{\mathbf{w}}_p$: weight vector having $\tilde{w}_i^p$ as components

$\tilde{E}(t)$: ideal eye velocity

$\dot{\tilde{E}}(t)$: time derivative of ideal eye velocity

$\tilde{S}(t)$: simple spike for inputting ideal eye velocity; this is referred to as ideal motor command in this paper

$x_i^m(t)$: firing rate of i-th MT, MST area cell with respect to m-th sample input

$u_{q,p}(j)$: $\|\mathbf{w}_q(j) - \tilde{\mathbf{w}}_p\| / \|\tilde{\mathbf{w}}_p\|$

3.2. Outline of model

Smooth pursuit eye movements of tracking a single target are simulated.

Figure 1 presents the overview of our model of smooth pursuit eye movements.

Since the direction selectivity of cells in the MST area has been discussed by the OFR model of Yamamoto et al. [16], this paper focuses its discussion on the velocity and acceleration selectivities and responses of the cells in the MT and MST areas. Considering a target moving left to right, the target velocity moving rightward is taken to be positive. MT, MST area cells responding to positive or negative target speeds are used.

First, assume that transformation from the firing rate $x_i(t)$ of an MT, MST area cell to a simple spike $S(t)$ is linear. Specifically, assume

$$S(t) = \sum_i w_i x_i(t) \tag{1}$$

Here, consider each Purkinje cell having the preferred direction in the rightward azimuth, and assume the spontaneous firing rates of $S(t)$ and $x_i(t)$ to be 0.

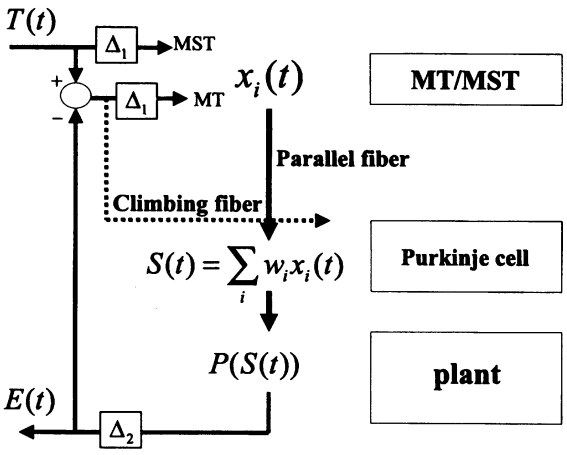

Fig. 1. A model of smooth pursuit eye movements.

Considering w_i to be the synapse weight between the parallel fiber and Purkinje cell, compute it according to feedback error learning

$$\frac{dw_i(t)}{dt} = \epsilon x_i(t - \delta_1)y(t) \quad (2)$$

$$y(t) = T(t - \delta_2) - E(t - \delta_2) \quad (3)$$

The weights before the beginning of learning are assumed to be 0. By learning, a simple spike is expected to become the motor command issued by the inverse dynamics model of a plant.

The eye velocity is computed by inputting a simple spike into the plant. Note that the plant takes the velocity as output in this paper. With s representing the variable in Laplace transformation, a plant is represented by a transfer function. The generality of the learning ability is shown by simulating three kinds of plants and the learning results are compared. The three plants are 1, $1/s$, and K. The Purkinje cell must learn their inverse, 1, s, and $1/K$. In other words, plant 1 and $1/s$ are used for extracting only the velocity information, acceleration information from the MT and MST activities.

In Section 3.3, a model for testing whether the target velocity and acceleration are extracted by feedback error learning or whether an inverse dynamics model of the control target can be learned is proposed. For this, its configuration is simplified such that the firing rate waveforms of the MT and MST area cells are linear sums of the target velocity and acceleration. In Section 3.4, a model incorporating more physiologically plausible conditions by reproducing various temporal waveform distributions of the firing rates of the MT and MST area cells is proposed.

3.3. Simple model

The model is simplified as follows. (1) Construct the firing rate waveforms of the MT and MST area cells from the linear sum or combinations of the target velocity and acceleration. (2) Assume that $\Delta_1 = 0$ ms, $\Delta_2 = 0$ ms. In other words, both the latent time until the firing of the MT and MST and the latent time until the eye movement are assumed to be 0 ms. (3) Assume $\delta_1 = 0$ ms and $\delta_2 = 0$ ms. In other words, time differences in learning are not considered.

The target velocity reaching a normal velocity after acceleration for a certain time is taken as the input to the MT and MST areas [acceleration times (50, 100, 150, 200 ms) and normal velocities (+10, +20, +30 deg/s) are combined randomly]. Next, construct the MT and MST area cell firing rate waveforms from linear sums of the target velocity and acceleration. Taking the maximum value (30 deg/s) of the velocity and the maximum value (600 deg/s^2) among the stimuli given to be 1, respectively, normalize the velocity and the acceleration of the input. The normalized velocity and acceleration with weights applied from 0 to 1 in 0.2 increments (0.0, 0.2, 0.4, 0.6, 0.8, 1.0) appropriately are taken as normalized firing rates of the MT/MST area cells. (Number of kinds of weights)^2 – 1 = 35 kinds of cells are used. Figure 2 shows examples of temporal waveforms of the firing rates. The inputs are target velocities that become the normal velocity of 20 deg/s after 100 ms acceleration. The horizontal axis of the lower right rectangle is the normalized firing rate and the vertical axis is the time (unit being milliseconds).

Taking the simulation of 1000 ms from inputting of the target velocity until outputting of the eye velocity as one trial, learning of a total of 5000 trials was performed.

The learning coefficients when the plants are 1, $1/s$, and K are assumed to be 3.0×10^{-4}, 5.0×10^{-7}, and 1.0×10^{-5}, respectively.

3.4. Physiologically plausible model

The following four points are incorporated into the model.

(1) Create MT and MST area cells having target velocity selectivities and different responses even with respect to accelerations (Fig. 3). Lisberger and Movshon's methods [2] were referenced. In Fig. 3, $f_j(x) = a_j \exp[-\{\log(x/v_j)/(b_j + c_j \log(x/v_j))\}^2]$. In addition, with $\delta = 1$, $a_1 = 10$, $b_1 = 400$ spikes/s, $c_1 = 1$, $d_1 = 0.03$, $v_1 = \{3$ deg/s each from 3 deg/s to 60 deg/s$\}$, and $a_2 = 100$, $b_2 = \{0.05, 0.5, 1, 5, 10\}$, $c_2 = 1$, $d_2 = 0.1$, $v_2 = v_1 + 10$, cells having 100 kinds of dynamics were used. The preferred stimulus velocity increases as v_1 and b_2 increase; the preferred stimulus velocity is scattered between 1 deg/s and 60

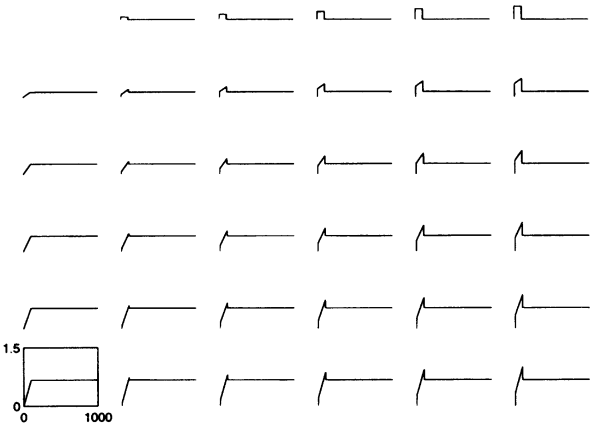

Fig. 2. An example of neuronal responses in area MT/MST constructed from linear combination of target velocity and acceleration.

deg/s. Here, in order to eliminate the effect of cell firing on the acceleration, the cell preferred stimulus velocity is defined as follows, following Lisberger and Movshon [2]: "It is assumed that the target velocity is step input. Among these, the target velocity that maximizes the averaged cell firing rates between 256 ms and 512 ms is taken as the preferred stimulus velocity."

(2) In order to reproduce the firing rate waveforms of the MT area cells in the state in which the eyes are actually moving, the retinal slip is input into the MT area. Lisberger and Movshon [2] presented an equation for creating the firing rate waveforms of the MT area cells in the state in which the eyes are not moving, taking the target velocity as input. Thus, replacing the input in Lisberger and Movshon's equation with the retinal slip is considered to be useful in reproducing the firing rate waveforms of the MT area cells of the state in which the eyes are actually moving. On the other hand, assuming that information that the MST area has other than visual stimuli as the target velocity, the target velocity is directly input into the MST area. By this, the firing rate waveforms of the MST area cells that keep firing by inputs other than visual stimuli observed by the physiological experiments of Newsome and colleagues [12] are modeled. Figure 4 shows an example of the firing rate waveforms of the MT and MST area cells. The plants in this case are K, and the waveforms are temporal waveforms of the firing rate of the case (Fig. 9A) of following a target that obtains a normal velocity of 20 deg/s after acceleration for 100 ms after learning. The parameters of A to D of Fig. 4 are the same and there are a total of 400 cells for which the input is of four kinds: a positive target velocity (Fig. 4A), positive retinal slip (Fig. 4B), negative target velocity (Fig. 4C), negative retinal slip (Fig. 4D). Because of the input of a positive target velocity, the cells of Fig. 4C do not fire. The horizontal axis of the lower left rectangle of Fig. 4D is the firing rate (spikes/s), and the vertical axis is the time (ms). The cells surrounded by the rectangle of Fig. 4A has the preferred stimulus velocity of 20 deg/s.

(3) $\Delta_1 = 65$ ms and $\Delta_2 = 10$ ms are assumed. Specifically, the time delay of 75 ms until the eyes start to move is considered.

(4) $\delta_1 = 250$ ms and $\delta_2 = 65$ ms are assumed. Specifically, time differences in learning are considered. In order to explain the effects of time differences in learning, the ideal eye velocity $\tilde{E}(t)$is defined as follows (Fig. 5A):

$$\tilde{E}(t) = T(t - 75) \tag{4}$$

Here, 75 ms is the time until the eyes start to move. Learning progresses in proportion to the amount of the climbing fiber input multiplied with the parallel fiber input delayed by 250 ms [Eq. (2)]. This is based on the consideration of the physiological experiments that have found that the learning effect is highest when the parallel fiber input and the climbing fiber input delayed by 250 ms interfere at a certain point in time [19]. When learning progresses and the ideal eye velocity is output, the climbing fiber input $T(t - 65) - \tilde{E}(t - 65)$ and the parallel fiber input delayed 250 ms do not overlap in time and a change greater than this does not occur (Fig. 5B). If there are no time differences in learning, the correlation between the climbing fiber input and the parallel fiber input $x_i(t)$ usually becomes positive and the weight continues to increase. On the one hand, since the retinal slip becomes equal to the target velocity at the beginning of learning and the parallel fiber input and the climbing fiber input overlap in time even when there are differences in learning, learning progresses (Fig. 5C).

After acceleration of a certain time, the target velocity reaching the normal velocity [the acceleration time (less

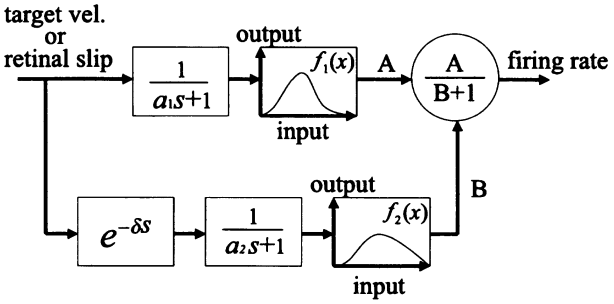

Fig. 3. Block diagram used to simulate responses of MT and MST neurons in the physiologically plausible model.

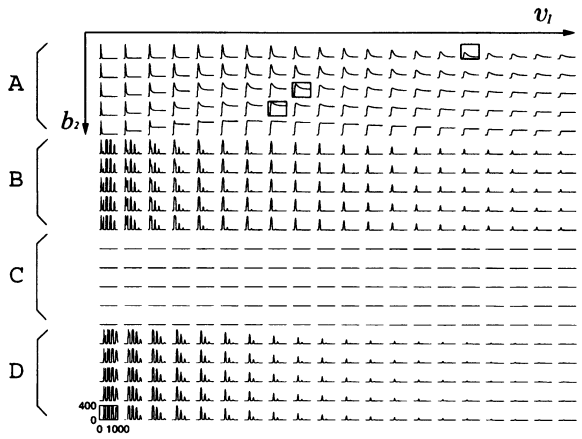

Fig. 4. An example of neuronal responses in area MT/MST based on Lisberger and Movshon's model [2].

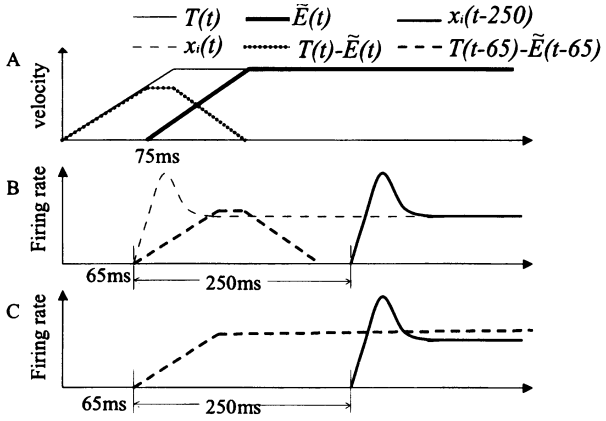

Fig. 5. Schematic diagram showing an effect of time difference between parallel fiber inputs and climbing fiber inputs during feedback error learning.

than 200 ms) and the normal velocity (+30 deg/s) combined randomly] is followed and learning is performed by trials of 10,000 times. The learning coefficient ε is 1.0×10^{-8}, 5.0×10^{-10}, and 1.0×10^{-9} when plants are 1, 1/*s*, and *K*, respectively.

In order to quantitatively discuss the learned weight or load, the optimal weight vector for outputting the ideal eye velocity when plants are *p* (1, 1/*s*, or *K*)

$$\tilde{\mathbf{w}}_p = (\tilde{w}_1^p \quad \tilde{w}_2^p \quad \ldots \quad \tilde{w}_N^p)^T \tag{5}$$

is computed and compared. Here, N (= 400) is the number of synapses. Specifically, $\tilde{\mathbf{w}}_p$ that minimizes

$$J = \|A\mathbf{w} - \mathbf{b}_p\|^2 + k\|\mathbf{w}\|^2 \tag{6}$$

is computed. As explained later, vector $\mathbf{b}_p$ is the ideal motor command when the plant is *p* [the simple spike for outputting the ideal eye velocity (Fig. 5A) is called this]. In addition, $A\mathbf{w}$ represents the simple spike when the weight is $\mathbf{w}$. Thus, the first term of J requires that $\mathbf{w}$ that issues the ideal motor command be determined. In addition, the second term is the normalization term that requires that the norm of the weight be large. This is the term added since the norm of the weight is predicted to be large since the feedback error learning of this paper is the gradient method and the weight only changes slowly and the initial value of the weight is 0.

$\tilde{\mathbf{w}}_p$ is computed as follows. M is assumed to be the number of kinds of sample target velocities. Here, M = 24 by combining 4 kinds of acceleration time (50, 100, 150, 200 ms) and 6 kinds of normal velocity (±10, ±20, ±30 deg/s). $\tilde{S}_p^m(t)$ is the ideal motor command when the plants are *p* and the target velocity is *m*. Specifically, $\tilde{S}_1^m(t) = \tilde{E}_m(t + \Delta_2)$ when plants are 1, $\tilde{S}_{1/s}^m(t) = \tilde{E}_m(t + \Delta_2)$ when plants are 1/*s*, and $\tilde{S}_K^m(t) = \mathcal{L}^{-1}(K^{-1}(\mathcal{L}(\tilde{E}_m(t + \Delta_2))))$ when plants are *K*. Defining vector $\mathbf{b}_p$ and matrix A as

$$\mathbf{b}_p = (\tilde{S}_p^1(0) \quad \tilde{S}_p^1(1) \quad \ldots \quad \tilde{S}_p^1(1000) \quad \tilde{S}_p^2(0) \quad \ldots \quad \tilde{S}_p^M(1000))^T \tag{7}$$

$$A = \begin{pmatrix} x_1^1(0) & x_2^1(0) & \ldots & x_N^1(0) \\ x_1^1(1) & x_2^1(1) & \ldots & x_N^1(1) \\ \vdots & \vdots & \ddots & \vdots \\ x_1^1(1000) & x_2^1(1000) & \ldots & x_N^1(1000) \\ x_1^2(0) & x_2^2(0) & \ldots & x_N^2(0) \\ \vdots & \vdots & \ddots & \vdots \\ x_1^M(1000) & x_2^M(1000) & \ldots & x_N^M(1000) \end{pmatrix} \tag{8}$$

$\tilde{\mathbf{w}}_p$ that minimizes J based on an appropriate k

$$\tilde{\mathbf{w}}_p = (A^T A + kI)^{-1} A^T \mathbf{b}_p \tag{9}$$

can be computed. Assume k = 200 when plants are 1 and K and k = 300 when plants are 1/*s*. In order to show that the weight approaches $\tilde{\mathbf{w}}_p$ as learning progresses, changes are followed by the number of times of trials of

$$u_{q,p}(j) = \|\mathbf{w}_q(j) - \tilde{\mathbf{w}}_p\| / \|\tilde{\mathbf{w}}_p\| \tag{10}$$

with the vector of the weight after *j* trials by feedback error learning when plants are *q* (1, 1/*s*, or *K*) as $\mathbf{w}_q(j)$.

4. Simulation Results

4.1. Simple model

Figure 6 shows the simulation results. The simple spikes are shown in units appropriate for the plants. Here, the simple spike when the eye velocity becomes equal to the target velocity is called the theoretically determined motor command. The simple spike (Fig. 6B) when the plants are 1 (Figs. 6A, B, C) becomes the target velocity (Fig. 6A). The simple spike (Fig. 6E) when the plants are 1/*s* becomes the target acceleration (Figs. 6D, E, F). In all cases, the simple spike becomes the theoretically determined motor command that the inverse dynamics model of the plants computes. The simple spike (solid line in Fig. 6H) is a good approximation of the theoretically determined

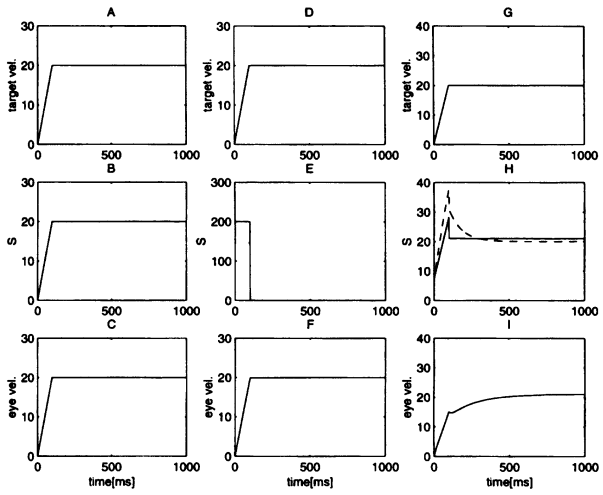

Fig. 6. Simulation results of the simple model.

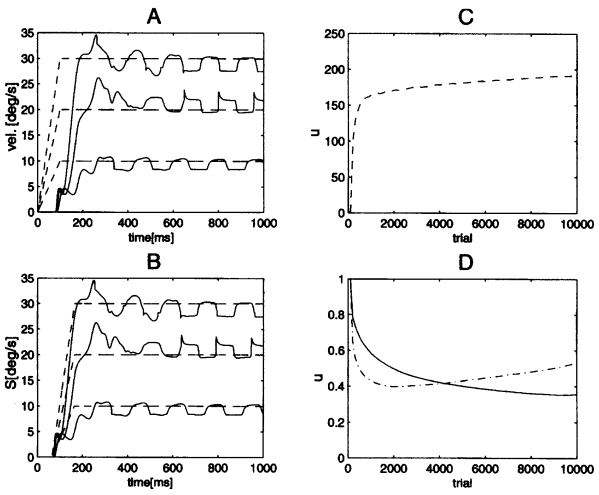

Fig. 7. Simulation results of the physiologically plausible model: plant 1.

motor command (broken line in Fig. 6H) for K plants. Thus, the eye velocity (Fig. 6I) becomes an approximation of the target velocity (Fig. 6G). The efficacy of feedback error learning has been shown by this model.

4.2. Physiologically plausible model

Figure 7 shows the results for one plant. The simple spike is shown in a unit appropriate for the plant (similarly for other plants below). The simple spike (solid line in Fig. 7B) obtained by learning becomes an approximation of the ideal motor command (broken line in Fig. 7B). Specifically, the eye velocity (solid line in Fig. 7A) can track the target velocity (broken line in Fig. 7A). Figures 7C and D show changes by the number of trials of $u_{1,p}(j)$. The data are plotted for every 100 trials. The solid line, broken line, and one dot chain line of Figs. 7C and D are $u_{1,1}$, $u_{1,1/s}$, and $u_{1,K}$, respectively. Since $u_{1,1}$ approaches 0 with learning, the weight approaches the optimal value $\tilde{\mathbf{w}}_1$.

Figure 8 shows the results for $1/s$ plant. The simple spike (solid line in Fig. 8B) obtained by learning is not the ideal motor command (broken line in Fig. 8B). This is due to the fact that first-order filters are used in the velocity input in creating the MT and MST area cell firing rate waveforms (Fig. 3) and there are no rapidly rising firing rate waveforms. However, learning is done such that the surface area is the same, and the eye velocity (solid line in Fig. 8A) ends up tracking the target velocity (broken line in Fig. 8A). Specifically, it can be said that the acceleration information necessary for the eye movement is extracted from the distribution of firing rate waveforms. Figure 8C shows changes for 100 trials each of $u_{1/s,p}(j)$. The solid line, broken line, and one dot chain line are $u_{1/s,1}$, $u_{1/s,1/s}$, and $u_{1/s,K}$ respectively. Here, the solid line and the one dot chain line overlap since $u_{1/s,1}$ and $u_{1/s,K}$ are almost 1. Since $u_{1/s,1/s}$ approaches 0 as learning progresses, the weight approaches the optimal value $\tilde{\mathbf{w}}_{1/s}$. However, the fact that $u_{1/s,1/s}$ does not decrease for other plants is due to the fact that there is a redundancy in constructing waveforms such as the solid line of Fig. 8B from the weighted linear sum since comparatively many cells react to acceleration and show transiently rising firing rate waveforms (Fig. 4).

Figure 9 shows the results for K plants. The simple spike (solid line in Fig. 9B) obtained by learning becomes

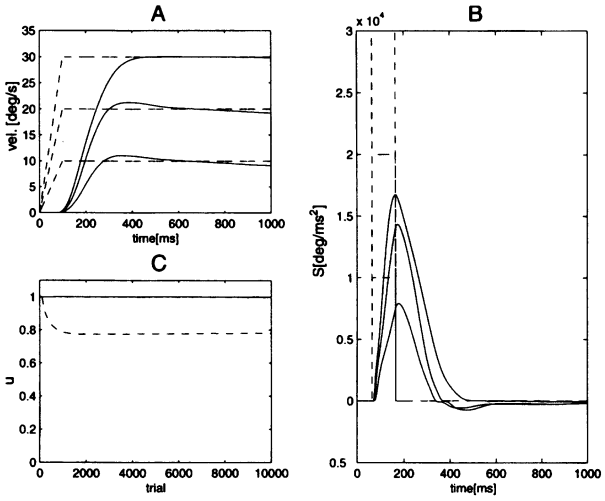

Fig. 8. Simulation results of the physiologically plausible model: plant $1/s$.

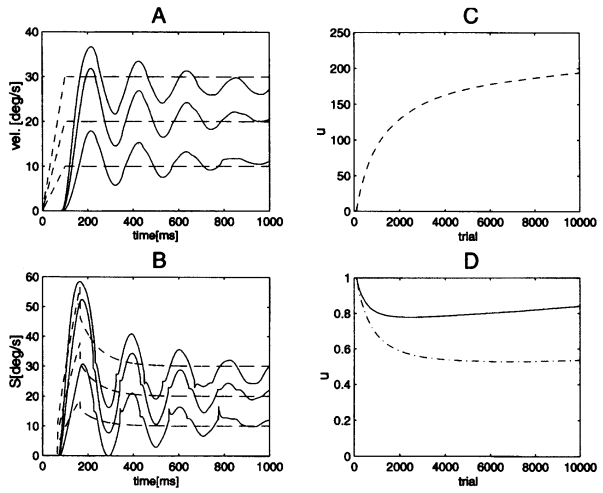

Fig. 9. Simulation results of the physiologically plausible model: plant K.

an approximation of the ideal motor command (broken line in Fig. 9B). Thus, the eye velocity (solid line in Fig. 9A) can track the target velocity (broken line in Fig. 9A). However, the point that the eye movement and oscillation in the simple spike is discussed in Section 5. Figures 9C and D show changes for 100 trials each of $u_{K,p}(j)$. The solid line, broken line, and one dot chain line of Figs. 9C and D are $u_{K,1}$, $u_{K,1/s}$, and $u_{K,K}$, respectively. It can be understood that the weight approaches the optimal value $\tilde{\mathbf{w}}_K$ from the fact that $u_{K,K}$ approaches 0 as learning progresses.

5. Discussion

5.1. Code transformation by learning

The model of this paper resolves insufficient aspects of Yamamoto's model [16] and Lisberger and Movshon's discussion [2]. The waveforms of the MT and MST activities having various temporal distributions of the state in which the eyes are in motion are reproduced. Specifically, the MST area having information on the target velocity and the MT area having information on the retinal slip are modeled, and cell groups having target velocity selectivities and differing responses to acceleration are used. In addition, since the model considers the delay time until the occurrence of the eye velocity, the inputs to the MT area are complicated and realistic. Thus, the simulation conditions for which appropriate motor commands cannot be obtained by simple linear sums of firing rate waveforms arise. Second, the weight is determined by feedback error learning by assuming that simple spikes can be reproduced from the weighted linear sums of the MT and MST area cell firing rates and assuming the weight to be the weight of the synapses between the parallel fiber input and Purkinje cells. Specifically, Yamamoto's model could be expanded to smooth pursuit eye movements, and transformation from population codes into firing codes could be done due to the synaptic plasticity of the cerebral cortex. Third, information on the velocity and acceleration necessary for eye movements could be selectively extracted from the MT and MST area cell firing rate waveforms by varying plants. For any plants, the weight approaches the optimal value by learning. This shows the generality of the learning capability.

Here, the results for K plants are further considered. The eye velocity and the simple spike fluctuate in the case of K plants. This is due to the fact that the weight is learned from 0 and the magnitudes of the synaptic weight that uses the MT area cell firing as input and the synaptic weight that uses the MST area cell firing as input are almost the same. Since the effect of the MT area, which is the feedback path having a delay, is excessive, unstable control results, leading to fluctuations in the eye velocity and simple spike. In addition, $u_{K,K}$ does not decrease as much as $u_{1,1}$ (one dot chain line, Fig. 9D). As measures for resolving this, varying the learning coefficients of the synaptic weight using the MT area cell firing as input and the synaptic weight using the MST area cell firing as input or varying the time and the intensity of the input into Purkinje cells such that the parallel fiber input from the MT area is dominant in the initial phase (the stage immediately after the target starts to move and the eyes accelerate quickly and track the target velocity) and the parallel fiber input from the MST is dominant in the maintenance phase (the stage after the initial phase when the eye velocity drops close to the target velocity), etc., are considered.

5.2. MST area model

The MST area is modeled by inputting the target velocity directly into the MST area in this paper. However, the input from the visual sensory system is only the retinal slip in the task of following one target by eyes with the head fixed. The following two hypotheses hold regarding the authors' MST area model. (1) Neuronal activities independent of the visual stimuli in the MST area are reproduced from only retinal slips. (2) The neuronal activities of the MST area predict the target velocity. Regarding this, Tabata and colleagues [20] reproduced neuronal activities independent of visual stimuli by simulating the neuronal field dynamics. In addition, Shibata and colleagues [21] constructed the MST area by a circulating connection type neuronal circuit and simulated smooth pursuit eye movements having the mechanism of predicting the target velocity. In addition, the authors implemented the model in a

humanoid eye system and showed the computer theoretical efficacy of the velocity prediction mechanism. The two hypotheses are shown to be theoretically feasible from these findings. Information other than visual stimuli in the MST area and the effects of this information on the population coding of visual stimuli remain to be experimentally clarified in the near future.

6. Conclusions

This paper discussed sensory movement transformation by modeling smooth pursuit eye movements. We plan to investigate optimal sensory movement transformation of the case considering noise in cell firing and its connection with learning of the cerebellum, and to develop theories that can be compared with the physiological and behavioral experiments of eye movements.

REFERENCES

1. Pouget A, Dayan P, Zemel R. Information processing with population codes. Nat Reviews Neurosci 2000;1:125–132.
2. Lisberger SG, Movshon JA. Visual motion analysis for pursuit eye movements in area MT of macaque monkeys. J Neurosci 1999;19:2224–2246.
3. Recanzone GH, Wurtz RH, Schwarz U. Responses of MT and MST neurons to one and two moving objects in the receptive field. J Neurophysiol 1997;78:2904–2915.
4. Salzman CD, Newsome WT. Neural mechanisms for forming a perceptual decision. Science 1994;264:231–237.
5. Georgopoulos AP, Schwartz AB, Kettner RE. Neural population coding of movement direction. Science 1986;233:1416–1419.
6. Groh JM, Born RT, Newsome WT. How is a sensory map read out? Effects of microstimulation in visual area MT on saccades and smooth pursuit eye movements. J Neurosci 1997;17:4312–4330.
7. Kawano K. Eye-movement related processings. In: Handbook for visual information processing. Asakura-Shoten; 2000. p 88–95. (in Japanese)
8. Kawato M. Internal models for motor control and trajectory planning. Curr Opin Neurobiol 1999;9:718–727.
9. Kawano K. Ocular tracking: Behavior and neurophysiology. Curr Opin Neurobiol 1999;9:467–473.
10. Komatsu H, Wurtz RH. Relation of cortical areas MT and MST to pursuit eye movements. I. Localization and visual properties of neurons. J Neurophysiol 1988;60:580–603.
11. Kawano K, Shidara M, Watanabe Y, Yamane S. Neural activity in cortical area MST of alert monkey during ocular following responses. J Neurophysiol 1994;71:2305–2324.
12. Newsome WT, Wurtz RH, Komatsu H. Relation of cortical areas MT and MST to pursuit eye movements. II. Differentiation of retinal from extraretinal inputs. J Neurophysiol 1988;60:604–620.
13. Shidara M, Kawano K. Role of Purkinje cells in the ventral paraflocculus in short-latency ocular following responses. Exp Brain Res 1993;93:185–195.
14. Gomi H, Shidara M, Takemura A, Inoue Y, Kawano K, Kawato M. Temporal firing patterns of Purkinje cells in the cerebellar ventral paraflocculus during ocular following responses in monkeys. I. Simple spikes. J Neurophysiol 1998;80:818–831.
15. Takemura A, Kobayashi Y, Kawano K. Roles of the cerebellum in smooth pursuit eye movements. Shinkei Shinpo 2000;44:734–747. (in Japanese)
16. Yamamoto K, Takemura A, Kawano K, Kobayashi Y, Kawato M. Computational simulation of transformation from visual inputs into motor command during ocular following responses. Tech Rep IEICE 1998;NC98-29:38–44.
17. Kobayashi Y, Kawano K, Takemura A, Inoue Y, Kitama T, Gomi H, Kawato M. Temporal firing patterns of Purkinje cells in the cerebellar ventral paraflocculus during ocular following responses in monkeys. II. Complex spikes. J Neurophysiol 1998;80:832–848.
18. Krauzlis RJ. Population coding of movement dynamics by cerebellar Purkinje cells. NeuroReport 2000;11:1045–1050.
19. Chen C, Thompson RF. Temporal specificity of long-term depression in parallel fiber-Purkinje synapses in rat cerebellar slice. Learning & Memory 1995;2:185–198.
20. Tabata H, Shibata T, Taguchi S, Kawato M. Simulation study on the smooth pursuit eye movement with MST-neural field model. Tech Rep IEICE 2001;NC2000-101:63–70.
21. Shibata T, Tabata H, Kawato M. Smooth pursuit oculomotor control based on learning a visual target dynamics, and its implementation on a humanoid. Tech Rep IEICE 2001;NC2000-100:55–62. (in Japanese)
22. Kawato M. Feedback-error-learning neural network for supervised motor learning. In: Eckmiller R (editor). Advanced neural computers. Elsevier; North-Holland; 1990. p 365–372.

AUTHORS (from left to right)


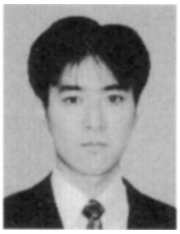

Shinya Taguchi (member) received his M.S. degree from the Department of Information Science, Nara Institute of Science and Technology, in 2002. He is currently responsible for a mobile image processing system at Mitsubishi Electric Corporation Information Technology R&D Center.

Hiromitsu Tabata (member) received his B.S. degree from Osaka University in 1998 and Ph.D. degree in engineering from Nara Institute of Science and Technology (NAIST) in 2002. He was a member of the emergency technical staff, with the Kawato Dynamic Brain Project, ERATO, Japan Science and Technology Corporation, from 1999 to 2001. He has been a research fellow of the Japan Society for Promotion of Science since 2001. He received a 2002 best student award at NAIST, 2003 research promotion award, Society of Instrument and Control Engineers. His research interests include theoretical and experimental studies using the eye movement system. He is a member of the Society for Neuroscience, Japanese Society for Neuroscience, and Society of Instrument and Control Engineers.

Tomohiro Shibata (member) received his B.E., M.E., and Ph.D degrees in information engineering from the University of Tokyo in 1991, 1993, and 1996. From 1996 to 1997, he was a postdoctoral fellow at the University of Tokyo. From 1997 to 2001, he was a researcher with the Kawato Dynamic Brain Project, ERATO, Japan Science and Technology Corporation (JST). From 2001 to 2002, he was a researcher of Metalearning, Neuromodulation and Emotion, Creating the Brain, CREST, JST. Currently he is an associate professor in the Graduate School of Information Science, Nara Institute of Science and Technology. He received the young investigator award from the Robotics Society of Japan in 1992, and the best paper award from the Japan Neural Network Society in 2002. He is a member of the Society for Neuroscience, IEICE, Japan Neural Network Society, and Robotics Society of Japan.

Mitsuo Kawato (member) received his B.S. degree in physics from the University of Tokyo in 1976 and M.E. and Ph.D. degrees in biophysical engineering from Osaka University in 1978 and 1981. From 1981 to 1988 he was a faculty member and lecturer at Osaka University. In 1988 he moved to ATR Auditory and Visual Perception Research Laboratories, Cognitive Processes Department, as a senior researcher. In 1992 he became a department head of Department 3, ATR Human Information Processing Research Laboratories. He has been Director of ATR Computational Neuroscience Laboratories since 2003. From 1996 to 2001 he was jointly appointed as a director of the Kawato Dynamic Brain Project, ERATO, JST. He has been jointly appointed as a visiting professor at the Kanazawa Institute of Technology, Nara Institute of Science and Technology, and Osaka University. For the last 15 years he has been working in computational neuroscience. He was awarded the Yonezawa founder's medal memorial special award from IEICE in 1991, outstanding research award from the International Neural Network Society in 1992, Osaka Science Prize in 1993, 10th Tsukahara Naka-akira Memorial Award in 1996, and Tokizane Toshihiko memorial award. He is a governing board member of the Japanese Society of Neuroscience and Japan Neural Network Society, and a member of the Executive Committee of the International Association for the Study of Attention and Performance.